Improved Magnetic STAR Methods for Real-Time, Point-by-Point Localization of Unexploded Ordnance and Buried Mines

Roy Wiegert, Kwang Lee and John Oeschger
NSWC PCD, Panama City, Florida

Abstract- **There is a pressing need for a practical and effective magnetic sensing technology that can be deployed onboard highly maneuverable sensing platforms and used for real-time, point-by-point detection, localization and classification (DLC) of magnetic targets such as ferrous unexploded ordnance (UXO) e.g., bombs, buried mines and artillery shells. Therefore the Strategic Environmental Research and Development Program (SERDP) has supported research and development, by Naval Surface Warfare Center Panama City Division (NSWC PCD), of a novel man-portable Magnetic Scalar Triangulation and Ranging (i.e., "STAR" and/or "MagSTAR") technology for DLC of UXO. The STAR concept uses scalar magnitudes of magnetic gradient tensors to triangulate the locations of magnetic targets. The magnitudes are analogous to central potential-type functions and they can provide true point-by-point DLC capabilities for sensing platforms in general, unconstrained motion.**

A prototype man-portable STAR Gradiometer was designed and constructed at NSWC PCD to provide a completely portable and user-friendly technology for real-time DLC of magnetic UXO. The prototype STAR Sensor comprises: a) A cubic array of eight fluxgate magnetometers. b) A 24-channel data acquisition/signal processing system. In field tests the man-portable sensor has demonstrated very robust, motion-noise-resistant DLC performance against isolated dipole type targets .

This paper describes work that is ongoing to enhance the performance of the MagSTAR Technology. In particular, two improved algorithms for solving the "STAR Equations" are described: 1) A directional derivative (DD) method based on the fact that the gradient of a central potential field is a vector that points toward the target/source of the locally strongest gradient. 2) A least-squares-fit (LSF) method that iteratively calculates a magnetic target's location and magnetic signature. The DD method is being developed for better discrimination between multiple targets but for isolated targets it is more susceptible to sensor noise than the LSF method. The initial LSF method applies primarily to DLC of isolated dipole targets. Thus, the methods preferably should be used concurrently as complementary DLC modalities in environments that may be magnetically complex. These improved methods should help facilitate the transition of the STAR Technology from man-portable applications to applications using highly maneuverable autonomous sensing platforms for real-time "on the fly" DLC of magnetic targets such as UXO and buried mines.

I. INTRODUCTION

This paper describes recent improvements to a new man-portable magnetic sensor system technology that is being developed for real-time, point-by-point Detection, Localization and Classification (DLC) of magnetic Unexploded Ordnance (UXO such as bombs, artillery shells and buried mines. The new technology is being developed at Naval Surface Warfare Center Panama City Division under the sponsorship of the Strategic Environmental Research and Development Program (SERDP). In order to perform true point-by-point DLC of a magnetic dipole target, at every point (within the sensor-target DLC range) a mobile magnetic sensor system must be capable of determining "on the fly" six unknowns; namely three components of a magnetic target's vector position (***r***) and three components of its magnetic signature (***M***) [1-3]. The ***M***-vector relates to the size, shape and orientation of ferrous UXO, thus measurements of ***M*** can be used to classify a magnetic target [4]. The present development of a portable technology for true real time point-by-point determination of ***r*** and ***M*** from sensing platforms in arbitrary, unconstrained motion is based on a multi tensor magnetic "Scalar Triangulation and Ranging (STAR)" concept [1] that specifically was created to provide an improved, more motion-noise-resistant magnetic sensing technology for real–time mine countermeasures using highly mobile sensing platforms. In 2007 field tests of SERDP's man-portable sensor system against magnetic dipole targets have conclusively demonstrated the unique advantages of the STAR technology for highly maneuverable sensing platforms. Details of the prototype MagSTAR sensor's construction and operation were presented in [2,3].

FIG. 1. Prototype MagSTAR Sensor and screenshot of near real time DLC data.
(a) The prototype man-portable MagSTAR Sensor shown in the photo was constructed using off-the-shelf sensing elements and electronics hardware. Therefore, the sensor is heavier (weight = 17 kg (37 lb)) and larger (2.4 m (7.9 ft)) long) than optimal. A next-generation "Mark II" MagSTAR Sensor could be made much smaller.
(b) Screenshot from operator's display showing range, bearing, elevation and magnetic signature of a 14.5 Am^2 magnetic dipole target. A UXO-type target's DLC data are correlated with the sensor's GPS data and presented on a heads-up display within 4 seconds after being measured by the sensor array.

FIG. 1a represents a typical test scenario with the prototype MagSTAR sensor being carried in the vicinity of a simulated target. FIG. 1b is a screenshot of DLC data that were presented in near real-time (within a total delay time of 4 seconds) on the operator's display as the sensor was swept past a 14.5 Am^2 magnetic dipole target (a small permanent magnet) that was used to simulate medium-sized UXO. Note that M =14.5 Am^2 is equivalent to the magnetic signature that an Earth's field of 50,000 nano-Tesla (nT) would induce in a ferrous, high-permeability sphere with a volume of 0.029 m^3 (1.02 ft^3). Field tests of the prototype STAR Sensor system have consistently demonstrated near real-time, point-by-point DLC at ranges of 5 to 7 m from the 14.5 Am^2 target.

The R&D effort in 2007 provided conclusive proof-of-principle of the magnetic STAR concept and demonstrated the world's first successful man-portable magnetic sensor system technology for real-time point-by-point DLC of magnetic targets. In 2008, the MagSTAR Project has focused on: 1) Optimizing the prototype sensor to improve its real-time performance against isolated dipole targets and, 2) Upgrading the prototype sensor to develop a new technology capable of performing effective DLC of UXO located in a cluttered field of magnetic anomalies. On continuation this paper will present details of two new STAR-based algorithms that are being developed as part of the ongoing optimization/upgrade process.

II. TENSOR GRADIOMETRY AND STAR THEORY

Detailed descriptions of the Magnetic Scalar Triangulation and Ranging (STAR and/or "MagSTAR") concept and STAR sensor construction are provided in [1-3]. The following brief review of tensor gradiometry and "STAR Theory" is presented for convenience in understanding the improved algorithms that are the subject of this paper. Tensor gradiometry is based on the following:

- The magnetic dipole equation for the magnetic anomaly field ($\boldsymbol{B}(\boldsymbol{r}, \boldsymbol{M})$ (in units of Tesla (T)) that emanates from a magnetic target:

$$\boldsymbol{B}(\boldsymbol{r}, \boldsymbol{M}) = (\mu/4\pi)[\, 3(\boldsymbol{M}\bullet\boldsymbol{r})\boldsymbol{r}/r^5 - \boldsymbol{M}/r^3]. \quad (1)$$

Where "$\boldsymbol{r}$" is the target's location vector, "$\boldsymbol{M}$" its magnetic dipole moment (amperes x meters squared =Am^2) and, for non magnetic media, the magnetic permeability $\mu \approx 4\pi$ x 10^{-7} Tm/A.

- The gradient of the target's field ($\boldsymbol{G} = \nabla\boldsymbol{B}$) is a tensor whose components (G_{ij}) are given by:

$$G_{ij} \equiv (\nabla\boldsymbol{B})_{ij} \equiv \partial B_i/\partial r_j = -3\ (\mu/4\pi)\ [\boldsymbol{M}\bullet\boldsymbol{r}(5r_ir_j - r^2\delta_{ij}) - r^2(r_iM_j + r_jM_i)]\ r^{-7} \quad (2)$$

The i, j represent components in a Cartesian (XYZ) coordinate system and $\delta_{ij} = 1$ for i = j, $\delta_{ij} = 0$ for i ≠ j.

Conventional tensor gradiometry essentially performs DLC by solving (2) for $\boldsymbol{r}$ and $\boldsymbol{M}$. However, Eq. (2) actually only represents a set of 5 independent equations that do not provide sufficient information for true point-by-point determination of the 6 unknown quantities represented by $\boldsymbol{r}$ and $\boldsymbol{M}$. As a result of this and other limitations [1,2], in order to localize and classify magnetic targets conventional tensor gradiometry typically requires platform motion to be constrained to nearly straight-line motion with relatively small changes in orientation. The MagSTAR concept was created to provide an improved magnetic gradient sensing technology for real-time, true point-by-point DLC with no constraints on sensing platform motion. STAR gradiometry is based on the following:

- The magnitude (C_T) of $\boldsymbol{G}$ is a robust, rotationally invariant scalar quantity equal to the square root of the "tensor contraction" or trace of $\boldsymbol{G}\bullet\boldsymbol{G}^{transpose}$. Furthermore, the relation between C_T, r and M can also be written in a form that's analogous to that of a central-potential-type scalar function, that is:

$$C_T = |\boldsymbol{G}| = [\Sigma\,(G_{ij})^2]^{0.5} = k(\mu/4\pi)M/r^4 \qquad (3)$$

where "k" is an "asphericity parameter"− a number that slowly varies from about 7.2 for field points aligned with the target's dipole axis to 4.2 for points transverse to the dipole axis [1,6]. The equation $C_T = k(\mu/4\pi)M/r^4$ constitutes the basic "STAR Equation" that provides the mathematical basis for triangulation of magnetic targets. FIG. 2 illustrates the geometrical nature of the C_T field that surrounds magnetic dipole targets. The MagSTAR Technology exploits the following characteristics of the C_T-field:

- Contours of C_T = constant form concentric spheroidal "equipotential-type" surfaces that are centered on a magnetic target.
- For a given value of k, differences in C_T values relate only to differences in r-values between the target and the respective C_T-measurement points. Thus, if C_T is measured at multiple points within a STAR gradiometer array with cubic symmetry:

a) The distances (ΔS_X, ΔS_Y, ΔS_Z) between C_T-measurement points constitute "triangulation baselines" that are determined by the geometrical design of the gradiometer.

b) The triangulation baselines, their respective end-point C_T values and (3) can be used in a STAR Algorithm to triangulate XYZ components of $\boldsymbol{r}$[1].

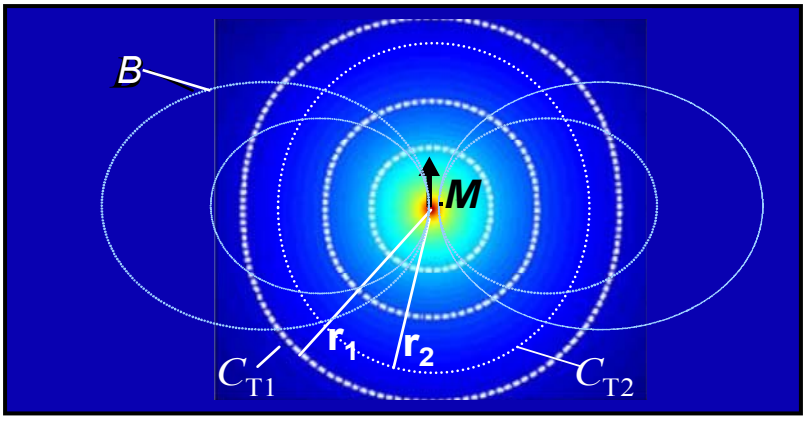

FIG. 2 Theoretical representation of the C_T field of a magnetic target

Two-dimensional (2-D) representation of geometrical relations between a magnetic target with dipole signature $\boldsymbol{M}$, the 3-D magnetic anomaly field ($\boldsymbol{B}$) that emanates from $\boldsymbol{M}$ and the target's 3-D C_T –field (with relative intensities represented by shaded colors ranging from dark red (0 dB) to dark blue (-90 dB)). White dotted lines highlight a set of curves with constant C_T's. Ratios of C_T-parameters are used to triangulate the location $\boldsymbol{r}$ of a magnetic UXO-type target.

FIGs. 3−5 present an overview of the Magnetic STAR's approach to solution of the problem of localization and classification of UXO. The improved magnetic STAR-based DLC methods described below involve the application of one or both of two novel approaches: 1) A directional derivative (DD) method, 2) A least squares fit (LSF) method. In contrast to the original STAR approach [1], the improved methods have the advantages that they provide better DLC accuracy for any orientation of the sensor array and enable development of improved modalities for DLC of UXO in magnetically cluttered environments.

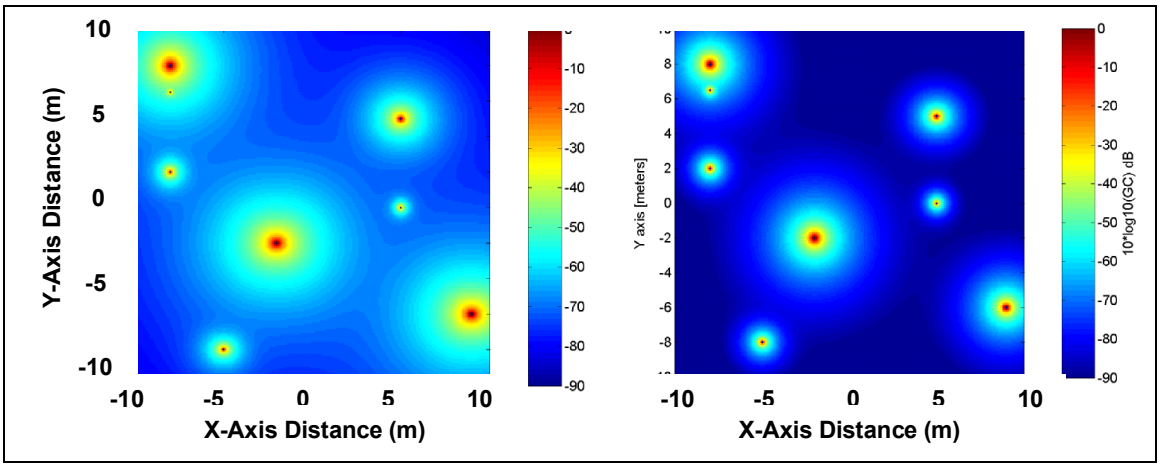

FIG. 3. Theoretical representations of magnetically cluttered STAR fields and their gradients. Left side: Cluttered C_T field from UXO-type targets with dipole moments ranging from 0.044 Am^2 to 37 Am^2. Overlapping C_T fields between targets will cause inaccuracies in the original STAR method. Right side: Gradient (∇C_T) of the cluttered C_T field. The ∇C_T function reduces the effect of overlapping anomaly fields and provides the basis for the "directional derivative (DD)" STAR method.

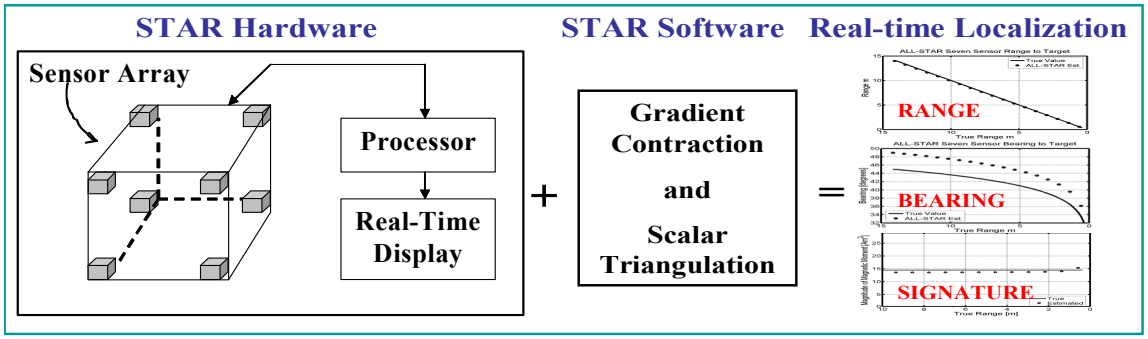

FIG. 4. Simplified illustration of design and operation of a cubic STAR sensor. A cubic array (shaded boxes) of eight low noise Triaxial Fluxgate Magnetometers (TFM) develops 24 channels of vector ***B***- field data. Processor hardware/software develops motion-compensated tensor and scalar data and runs a STAR Algorithm to provide a real-time, point-by-point display of vector components of target range ***r***, and magnetic signature ***M***.

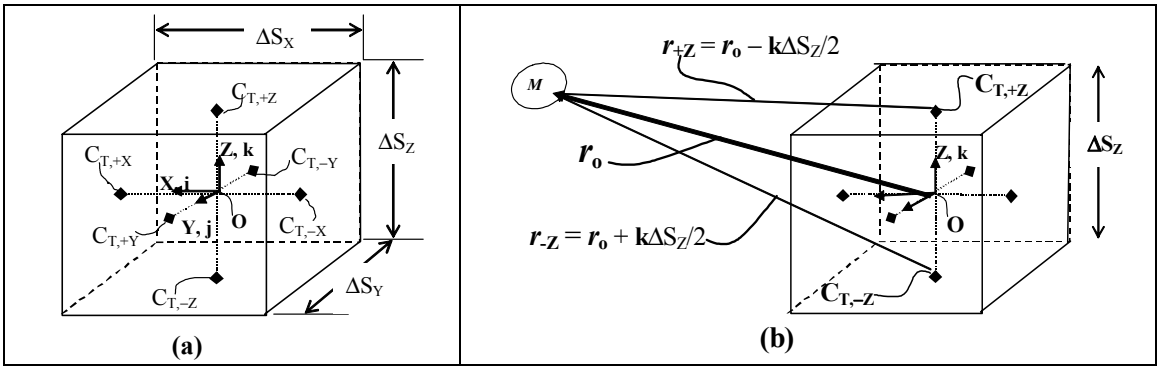

FIG. 5. Definition of coordinate system and triangulation parameters for a cubic STAR sensor. (a) A Cartesian (XYZ) coordinate system with unit vectors **i, j, k** is located at the center of symmetry (O) of a cubic array of TFMs that provides the "framework" for an array of $C_{T,\,I}$ parameters and triangulation baselines ΔS_X, ΔS_Y and ΔS_Z. For clarity of illustration, the TFMs at the vertices of the cube are not shown. (b) Relation between the sensor-target vector $\boldsymbol{r}_o$, vectors $\boldsymbol{r}_{+Z}$ and $\boldsymbol{r}_{-Z}$ from $C_{T,\,+/-Z}$ measurement points to target (***M***) and the triangulation baseline ΔS_Z. For clarity, the $\boldsymbol{r}_I$ vectors, $C_{T,\,I}$ measurement points and triangulation baselines corresponding to the X- and Y-directions are not shown.

III. DIRECTIONAL DERIVATIVE (DD) STAR METHOD

With reference to FIG. 4, the DD method comprises the following steps:

1) Calculation of the spatial gradient of C_T (∇C_T). The magnitude of ∇C_T is the value of the directional derivative of the function $C_{T,I} = (\mu/4\pi)kMr_I^{-4}$ in the direction of the greatest rate of change of C_T; that is, in the direction $\boldsymbol{r_o}$ toward the target. Thus, this step calculates $\nabla C_T \approx \mathbf{i}(\Delta C_{T,X}/\Delta S_X) + \mathbf{j}(\Delta C_{T,Y}/\Delta S_Y) + \mathbf{k}(\Delta C_{T,Z}/\Delta S_Z)$ where **i, j, k** are unit vectors along the sensor's XYZ axes and $\Delta C_{T,X} = (C_{T,+X} - C_{T,-X})$, etc. Note that ∇C_T is along the $\boldsymbol{r_o}$ vector and is measured with respect to the center of symmetry of the TFM sensor array.
2) Calculation of a unit vector $(\mathbf{U}_{\boldsymbol{ro}}) = \nabla C_T / |\nabla C_T|$ along the $\boldsymbol{r_o}$ vector to the target
3) Calculation of $\boldsymbol{r_I}$ vectors in terms of their respective triangulation baselines ΔS_i, r_o, unit vector $\mathbf{U}_{\boldsymbol{ro}}$ and XYZ unit vector (i.e., **i**, **j**, **k**). More specifically, this step involves calculations of scalar projections of triangulation baselines in the direction of the $\boldsymbol{r_o}$ vector to the target; namely, $\mathbf{U}_{\boldsymbol{ro}}\bullet\mathbf{i}\Delta S_X$, $\mathbf{U}_{\boldsymbol{ro}}\bullet\mathbf{j}\Delta S_Y$, and $\mathbf{U}_{\boldsymbol{ro}}\bullet\mathbf{k}\Delta S_Z$. For example $|\boldsymbol{r}_{+Z}| = |\boldsymbol{r_o} - \mathbf{k}\Delta S_Z/2|$, etc. Then it follows that for the r_{+Z} distance:
   a) $r_{+Z} = [\boldsymbol{r_o} - \mathbf{k}\Delta S_Z/2)\bullet(\boldsymbol{r_o} - \mathbf{k}\Delta S_Z/2)]^{0.5}$
   b) $= [r_o^2 - \boldsymbol{r_o}\bullet\mathbf{k}\Delta S_Z + (\Delta S_Z/2)^2]^{0.5}$
   c) $= r_o[1 - \mathbf{U}_{\boldsymbol{ro}}\bullet\mathbf{k}\Delta S_Z/r_o + (\Delta S_Z/2r_o)^2]^{0.5}$
   d) $\approx r_o - \mathbf{U}_{\boldsymbol{ro}}\bullet\mathbf{k}\Delta S_Z/2$
   e) also, $r_{-Z} = r_o[1 + \mathbf{U}_{\boldsymbol{ro}}\bullet\mathbf{k}\Delta S_Z/r_o + (\Delta S_Z/2r_o)^2]^{0.5} \approx r_o + \mathbf{U}_{\boldsymbol{ro}}\bullet\mathbf{k}\Delta S_Z/2 = r_{+Z} + \mathbf{U}_{\boldsymbol{ro}}\bullet\mathbf{k}\Delta S_Z$

Similar relations in terms of r_o, $\mathbf{U}_{\boldsymbol{ro}}$ and the respective baselines ΔS_i can be obtained for the magnitudes of the remaining projection distances r_{+Y}, r_{-Y}, r_{+Z} and r_{-Z}.

Next, at step 4) the STAR process described in [1,5] is applied using the gradient contraction $C_{T,I}$ parameters and the relations between r_I (and/or r_o) magnitudes and the respective r_I distances determined in steps 1) – 3). Thus, for the given example:

4) Application of the STAR process comprises:
   $r_{+Z}/r_{-Z} = r_{+Z}/(r_{+Z} + \mathbf{U}_{\boldsymbol{ro}}\bullet\mathbf{k}\Delta S_Z) = (C_{T,-Z}/C_{T,+Z})^{0.25}$
   $\rightarrow r_{+Z} = (\mathbf{U}_{\boldsymbol{ro}}\bullet\mathbf{k}\Delta S_Z)[(C_{T,+Z}/C_{T,-Z})^{0.25} - 1]^{-1}$
   $\rightarrow r_o = (\mathbf{U}_{\boldsymbol{ro}}\bullet\mathbf{k}\Delta S_Z)[(C_{T,+Z}/C_{T,-Z})^{0.25} - 1]^{-1} + 0.5\mathbf{U}_{\boldsymbol{ro}}\bullet\mathbf{k}\Delta S_Z$
   $\boldsymbol{r_o} = r_o\,\mathbf{U}_{\boldsymbol{ro}} = \{\mathbf{U}_{\boldsymbol{ro}}\bullet\mathbf{k}\Delta S_Z)[(C_{T,+Z}/C_{T,-Z})^{0.25} - 1]^{-1} + 0.5\mathbf{U}_{\boldsymbol{ro}}\bullet\mathbf{k}\Delta S_Z\}\mathbf{U}_{\boldsymbol{ro}}$
5) Calculation of r_{oX} , r_{oY} , r_{oZ} the XYZ components of $\boldsymbol{r_o}$, where: $r_{oX} = \boldsymbol{r_o}\bullet\mathbf{i}$; $r_{oY} = \boldsymbol{r_o}\bullet\mathbf{j}$, $r_{oZ} = \boldsymbol{r_o}\bullet\mathbf{k}$.
6) Calculation of XYZ components of $\boldsymbol{M}$ i.e., M_X, M_Y, M_Z by substitution of r_{oX}, r_{oY}, r_{oZ} into (2).

The resulting target parameters (e.g., $\boldsymbol{r_o}$ and $\boldsymbol{M}$ values) can be output to (i) a user display and/or (ii) another application. Note that for some applications the $\boldsymbol{r_o}$ values can also be conveniently expressed in spherical coordinates (e.g., r, θ, φ coordinates) in terms of the target's scalar range r_o, its elevation angle θ, and its bearing angle φ, relative to the sensor system. This angular representation is shown in FIG. 5 for θ and φ values obtained using the least squares fit method. Note that the DD method can use the ∇C_T function to narrow the sensor's field-of-view and thereby "sharpen" the sensor's target-discrimination capability. The use of both C_T– and ∇C_T–derived quantities allows development of a unique capability for discrimination of magnetic UXO and/or buried mines in magnetically cluttered environments. Thus, the DD method is being developed as a modality for localization and discrimination of targets in magnetically complex environments. In particular, even in the presence of magnetic clutter and/or non-dipolar sources, the directional derivative vector will point in the direction of the strongest field-gradients, i.e., toward the nearest and/or locally strongest magnetic anomaly/target.

IV. LEAST SQUARES FIT (LSF) STAR METHOD

When there is only a single magnetic dipole type target in the STAR Sensor's field-of-view, a simple nonlinear least-squares-fit (LSF) method may provide target localization results that are less susceptible to sensor system noise. The LSF method uses the gradient contraction $C_{T,I}$ parameters to self-consistently determine the set of XYZ components of $\boldsymbol{r_o}$ (i.e., r_{oX}, r_{oY}, r_{oZ}) that provide the best fit (in a least-squares sense) to a set of three of the $C_{T,I} = (\mu/4\pi)kMr_I^{-4}$ equations for the parameters $C_{T,+X}$, $C_{T,-X}$, $C_{T,+Y}$, $C_{T,-Y}$, $C_{T,+Z}$, $C_{T,-Z}$ and/or their ratios. For example, in terms of $\boldsymbol{r_o}$ (vector from center of array to target), unit vector **k**, and triangulation baseline ΔS_Z, the equation for $C_{T,+Z}$ can be expressed as follows:

$$C_{T,+Z} = (\mu/4\pi)kM\,[\,|\,(\boldsymbol{r_o} - \mathbf{k}\Delta S_Z/2)\,|\,]^{-4} = M'[r_o^2 - \boldsymbol{r_o}\bullet\mathbf{k}\Delta S_Z + (\Delta S_Z/2)^2]^{-2} = M'[r_o^2 - r_{oZ}\Delta S_Z + (\Delta S_Z/2)^2]^{-2}$$

where $r_o = [(r_{oX})^2 + (r_{oY})^2 + (r_{oZ})^2]^{0.5}$ and $M' \equiv (\mu/4\pi)kM$.
Specifically, the LSF method performs the following operations:

1) Selects a set of initial values for r_{oX}, r_{oY}, r_{oZ} in accordance with the "STAR constraint" discussed below.
2) Uses the r_{oX}, r_{oY}, r_{oZ} values in the $C_{T,\,I}$ equations to calculate a set of $C_{T,\,I}$ parameters and their ratios.
3) Calculates the sum of squares of the differences between the calculated $C_{T,\,I}$ values and the $C_{T,\,I}$ values that were measured by the sensor array.
4) Determines if the sum of squares is greater than a predetermined "tolerance parameter." If the sum of the squares is greater, the process goes to operation 5 described below. If the sum of the squares is less than or equal to the tolerance parameter, the process goes to operation 6 described below.
5) Applies a set of differential "adjustments" (Δr_{oX}, Δr_{oY}, Δr_{oZ}) to the r_{oX}, r_{oY}, r_{oZ} values and returns to operation 2. The differential adjustments can be determined by using a procedure such as Newton's root-finding method in combination with the "STAR constraint" described below.
6) Uses the LSF-determined r_{oX}, r_{oY}, r_{oZ} values in the gradient tensor equations to calculate the XYZ components of target signature vector $\boldsymbol{M}$.

With regard to the "STAR constraint" mentioned in operations 1 and 5 above, note that the $C_{T,\,I}$ equations are nonlinear polynomial equations of the fourth degree in the unknown quantity $\boldsymbol{r_o}$ and its components ($\mathbf{i}r_{oX}$, $\mathbf{j}r_{oY}$, $\mathbf{k}r_{oZ)}$. The existence of multiple roots for such an equation can lead to problems of convergence and/or uniqueness wherein multiple LSF-derived solutions may exist for a given set of $C_{T,\,I}$ parameters. In order to ensure rapid convergence of the LSF process to the one true position of the target, the following approach is used. For each set of C_T parameters, the processes of first selecting (operation 1) and then iteratively adjusting (operation 5) r_{oX}, r_{oY}, r_{oZ} preferably should be performed subject to a unique STAR-based constraint. The STAR constraint requires the components $\mathbf{i}r_{oX}$, $\mathbf{j}r_{oY}$, $\mathbf{k}r_{oZ}$, respectively, to be numerically proportional to, and to have the same sign as, the components of $\nabla C_T \approx \mathbf{i}(\Delta C_{T,\,X}/\Delta S_X) + \mathbf{j}(\Delta C_{T,Y}/\Delta S_Y) + \mathbf{k}(\Delta C_{T,Z}/\Delta S_Z)$. Then, the resultant LSF solution for $\boldsymbol{r_o}$ will be forced to be parallel to, and have the same sense as, ∇C_T and thereby uniquely correspond to the true position of the magnetic target.

FIG. 5 presents results from a LSF-type calculation of a target's relative bearing and elevation angles as the MagSTAR sensor was (a) held pointed at a magnetic dipole target and (b) swept back and forth past the target. Variations in the angular data in FIG. 5 result from a combination of unfiltered high-frequency noise and the difficulty of maintaining/moving the hand-held sensor at fixed angles during the field test. However, the preliminary results are very promising and further field testing (and simulations) soon will be done to establish a data base for complete characterization and optimization of the LSF and DD methods.

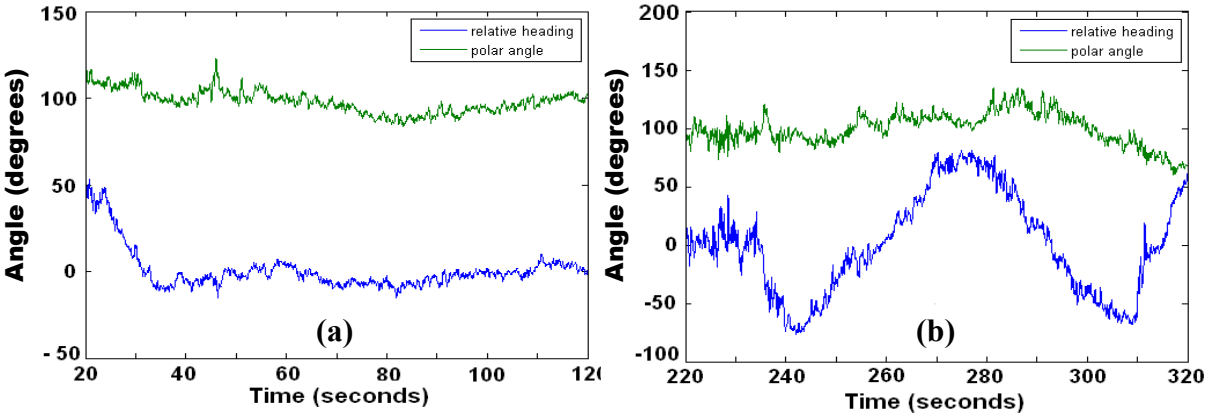

FIG. 5. Results of application of LSF method to STAR sensor data.
(a) Angular target-location data in MagSTAR coordinates (FIG. 4)) were calculated using a LSF approach for DLC data taken as the hand-held sensor was held pointed at a 14.5 Am^2 target located at a distance of about 5 m. The green (upper) data curve represents the target's polar angle (θ) (i.e., elevation) measured from the +Z direction. The blue (lower) data curve represents the target's bearing angle (φ) relative to the sensor's +X direction. In (b) upper and lower curves again respectively represent θ and φ. The sensor was initially pointed at the target, then the sensor's heading was swept about +/-75° past the target.

The $\boldsymbol{r_o}$ and $\boldsymbol{M}$ values independently determined by the DD and LSF methods can also be: 1) Correlated with one another as part the normal operation of the sensor system. 2) Further processed by a LSF-type method to eliminate the "asphericity errors" in $\boldsymbol{r_o}$ and $\boldsymbol{M}$ values that are caused by the C_T- fields' departure from perfect spherical symmetry [1]. It will generally not be known if a target is isolated or residing in a crowded field of magnetic anomalies; therefore, the STAR technology is currently being upgraded to include correlation of the results from the LSF and DD methods with each other and with the measurements of individual components of the MagSTAR sensor's six independently measured gradient tensors $\boldsymbol{G_I}$. This upgrade will include a more powerful data acquisition and signal processing system that will enhance the STAR technology's performance for DLC of UXO in magnetically complex environments.

V. Conclusion

Two novel algorithms have been developed for improving a MagSTAR sensor's detection, localization and classification (DLC) performance: 1) A directional derivative (DD) method based on the fact that the gradient of a central potential field is a vector that points toward the target/source of the locally strongest gradient. 2) A least-squares-fit (LSF) method that uses a unique "STAR constraint" to iteratively calculate a magnetic target's location and magnetic signature. The DD method appears to provide better discrimination between multiple targets while the initial LSF method applies primarily to DLC of isolated dipole targets. Thus, the methods preferably should be used concurrently as complementary DLC modalities in environments that may contain cluttered fields of magnetic anomalies. These improved methods should help facilitate the transition of the STAR Technology to a more general range of high-mobility sensing applications that require more effective discrimination of magnetic targets such as unexploded ordnance in magnetically complex environments.

Acknowledgment

This work was supported by the Strategic Environmental Research and Development Program (SERDP) under Project MM-1511. Fair winds and following seas to Dr. John Oeschger who, during his tenure at NSWC PCD, contributed greatly to the successful development of the Magnetic STAR technology.

References

[1] R.F. Wiegert and J. Oeschger, "Generalized Magnetic Gradient Contraction Based Method for Detection, Localization and Discrimination of Underwater Mines and Unexploded Ordnance," MTS/IEEE OCEANS 2005 Conference Proceedings.

[2] R.F. Wiegert and J. Oeschger, "Portable Magnetic Gradiometer for Real-Time Localization and Classification of Unexploded Ordnance," MTS/IEEE OCEANS 2006 Proceedings, September 2006.

[3] R.F. Wiegert, J. Oeschger and E. Tuovila, "Demonstration of a Novel Man-Portable Magnetic STAR Technology for Real-Time Localization of Unexploded Ordnance", MTS/IEEE OCEANS 2007 Proceedings, October 2007

[4] T.W. Altschuler, "Shape and Orientation Effects on Magnetic Signature Prediction for Unexploded Ordnance," UXO Forum 1996, (Williamsburg, VA, March 26-28, 1996), Conference Proceedings, pp.282-291.